




Article

Adsorptive of Nickel in Wastewater by Olive Stone Waste: Optimization through Multi-Response Surface Methodology Using Desirability Functions

Marina Corral Bobadilla ^{1,*}, Rubén Lostado Lorza ¹, Fátima Somovilla Gómez ¹ and Rubén Escribano García ²

¹ Department of Mechanical Engineering, University of La Rioja, 26004 Logroño, La Rioja, Spain; ruben.lostado@unirioja.es (R.L.L.); fatima.somovilla@unirioja.es (F.S.G.)

² LORTEK Technological Center, Basque Research and Technology Alliance (BRTA), Arranomendia Kalea 4A, 20240 Ordizia, Spain; escribano.engineer@gmail.com

* Correspondence: marina.corral@unirioja.es; Tel.: +34-941-299-274

Received: 30 March 2020; Accepted: 2 May 2020; Published: 7 May 2020



Abstract: Pollution from industrial wastewater has the greatest impact on the environment due to the wide variety of wastes and materials that water can contain. These include heavy metals. Some of the technologies that are used to remove heavy metals from industrial effluents are inadequate, because they cannot reduce their concentration of the former to below the discharge limits. Biosorption technology has demonstrated its potential in recent years as an alternative for this type of application. This paper examines the biosorption process for the removal of nickel ions that are present in wastewater using olive stone waste as the biosorbent. Kinetic studies were conducted to investigate the biosorbent dosage, pH of the solution, and stirring speed. These are input variables that are frequently used to determine the efficiency of the adsorption process. This paper describes an effort to identify regression models, in which the biosorption process variables are related to the process output (i.e., the removal efficiency). It uses the Response Surface Method (RSM) and it is based on Box Benken Design experiments (BBD), in which olive stones serves as the biosorbent. Several scenarios of biosorption were proposed and demonstrated by use of the Multi-Response Surface (MRS) and desirability functions. The optimum conditions that were necessary to remove nickel when the dosage of biosorbent was the minimum (0.553 g/L) were determined to be a stirring speed of 199.234 rpm and a pH of 6.369. The maximum removal of nickel under optimized conditions was 61.73%. Therefore, the olive stone waste that was investigated has the potential to provide an inexpensive biosorbent material for use in recovering the water that the nickel has contaminated. The experimental results agree closely with what the regression models have provided. This confirms the use of MRS since this technique and enables satisfactory predictions with use of the least possible amount of experimental data.

Keywords: biosorption; nickel; olive stone; multi-response surface methodology

1. Introduction

The control of water pollution has been of great interest for years due to its importance in protecting health and the environment. The discharge of untreated or insufficiently purified residual effluents is one of the main sources of water pollution. This is why much of the legislative actions in this matter by competent administrations have involved the control of discharges. It is sometimes difficult to compare the discharge limits with what conventional purification techniques achieve for the elimination of heavy metals. Thus, a search for techniques or procedures is necessary for reducing or eliminating

these types of emissions. In this context, biosorption research has shown, in recent years, the potential of this technology as an alternative method for the treatment of water that has been contaminated by heavy metals. The World Health Organization (WHO) has reported that all ecosystems and human health are threatened by serious exposures to heavy metals. The European Directive 2010/75/EU [1] listed manganese, lead, chromium, nickel, cadmium, zinc, copper, aluminum, mercury, and iron as heavy metals and pollutants for which emission limit values should be established.

Nickel is a widely used heavy metal in producing stainless steel, super alloys, and non-ferrous alloys. Nickel and its salts are also used in electroplating as a catalyst, in Ni-Cd batteries and in coins, welding products, electronic products, and some pigments. Consequently, nickel is used in numerous productive sectors, including construction, transportation, automotive, electronics, aeronautics, and telecommunications. A considerable amount will end up in the aquatic environment because there is very significant use of nickel in industry. The ingestion of nickel in excess of recommended levels is associated with severe lung and kidney damage, gastrointestinal problems, and shortness of breath, etc. [2].

Various methods for removing heavy metals from wastewater have been developed. They include physicochemical methods, such as chemical precipitation, oxidation-reduction, ion exchange [3,4], and various electrochemical treatments [5,6]. These include [6] ultrafiltration [7,8], photocatalysis [9], reverse osmosis [10,11], and electroflotation [12]. Their main drawback is that they are expensive and produce secondary sludge, which necessitates the use of additional treatment [13]. For this reason, there is a need for a method to remove metals from wastewater that is simple, efficient, and inexpensive. An adsorption process becomes a good option, since it is a simple method to remove metal ions from wastewater. However, the expense of using commercial adsorbents causes the use of the adsorption process to be costly. This has prompted the search for new strategies to develop low-cost materials that possess good removal capacity [14,15]. As a result of the above, agricultural and agro industrial wastes have been used as natural adsorbents for the elimination of heavy metals, due to their biodegradability, sustainability, and low cost. In addition, they offer the possibility of recovering the metal after the regeneration process, as well as enabling the recovery of waste [16,17]. Several materials, such as biosorbents, have been used. They are: bark [18], peat [19], various types of biomass [20,21], tobacco residues [22], algae [23], coffee residues and grape residues [24], grapefruit skin [25], and sugar-beet pectin [26]. Additionally, others materials that are based on biomass waste have been successfully used for the removal of nickel ions from wastewater. They include grape stem waste [27], rice straw [28,29], *Citrus Limettioides* carbon husk [30], lanzon [31], pineapple [32], cashew nut shell [33], spent mushroom substrate [34], *Litchi Chinensis* seeds [35], and olive mill waste [36].

Accordingly, this study seeks to investigate the optimization of the use of olive stone waste as a biosorbent agent for the removal of nickel from wastewater. With the growth of the olive oil industry, there has been a corresponding rise in the volume of olive mill waste production. Spain faces this problem. In recent years, the consumption of olive oil has increased significantly. This implies a proportional increase in olive mill wastes. In fact, Spain's oil produced is estimated to be 625,600 tons per year, according to a report that was published by the International Olive Council. Because of the increasing production of olive oil, olive mills face severe environmental problems, as olive mill waste management has no feasible and/or cost-effective response to the rising quantities of olive-mill waste. One interesting use of olive stone waste is as an inexpensive adsorbent in the removal of heavy metals from water. Various studies have been published on the subject of using solid waste products that the olive oil industry generates as adsorbents of heavy metals [36–38]. In conclusion, olive mill waste has a value due to its potential as a biosorbent agent. It represents a solution to the problem of waste disposal. The use of olive Stone waste as a biosorbent is supported by its properties. The chemical composition of olive stone waste mainly consists of lignin, cellulose, and hemicelluloses. The hydroxyl groups from the surface are the most abundant and reactive sites of the material and they can be used to incorporate a variety of functional groups. These active functional groups, including carbonyl and hydroxyl groups of the lignocellulosic material, interact with nickel ions throughout the adsorption

process [39,40]. It is known that removal efficiency is directly related to the content of the carboxyl groups in cellulose. Therefore, it is believed that adsorption occurs, in part, by ion exchange with carboxyl groups [41].

One of the most important problems facing the adsorption process is the search for the variables that will optimize this process. Optimizing the biosorption process requires identifying the process input variables that provide the greatest efficiency. In this context, it might be noted that the traditional method of experimentation involves only changing one factor at a time in the search for an optimal condition. This approach is known as one-variable-at-a-time. However, it does not determine the relationship among multi-variables because of the complexity of the influence of the factors. This approach is also lengthy, laborious, and costly, as many experiments must be undertaken. Multivariate statistics techniques enable the number of experiments to be reduced, as well as the impact of independent variables on the process. This aids in the development and optimization of the operating system. In turn, this greatly reduces the cost of experiments. Artificial intelligence techniques, such as Artificial Neural Network (ANN) and Response Surface Methodology (RSM), are frequently used to optimize the removal of heavy metals by biosorption. RSM provides mathematical statistical methodology with which to construct regression models (the functionality of second-order polynomials regression models) that effectively and efficiently analyze the effects of multiple variables [42]. There are three main steps in the process to remove heavy metals by biosorption while using the RSM. These appear in Figure 1. Several authors have optimized the removal of nickel from wastewater using RSM, by using different vegetable wastes as a biosorbent and with different input variables. For example, [43–45] studied the biosorption of Ni(II) in determining the efficiency of removal of Ni(II) while using RSM. These authors considered the stirring speed, pH, adsorbent dose, initial ion concentration, and temperatures as input variables. Bhagat et al. [46] recently reviewed some exclusive studies that were based on RSM. Other authors [37,38,47,48] also investigated the biosorption of Ni(II) using vegetable waste as a biosorbent. In most of these cited studies, the authors reported that the type and initial concentration of the adsorbent, pH, contact time, and mixing speed in heavy metal elimination. It is apparent that the input variables in the Ni(II) absorption processes in the previously mentioned research were mainly pH, stirring speed, and adsorbent dosage, no matter which biosorbent was used. These factors must be optimized before using olive stone as an adsorbent in order to increase the effectiveness of the nickel removal.

The main reason for the current research was to undertake a comprehensive study of optimization based on RSM with desirability functions, in which olive stone waste was used as an untreated biosorbent for the removal of Ni(II) from wastewater. In this research, the combined effects of biosorbent dosage (*bioDose*), pH (*pH*) and stirring speed (*S*) were considered as the input variables of the biosorption process, and the Ni(II) removal efficiency (*%NiR*) was considered as the output. The three steps that are described in Figure 1 were followed in the present study to obtain the optimal elimination of Ni(II) based on RSM. They were developed, as follows: regression models that address the efficiency of the removal process were created by the use of RSM that was based on experiments involving a Box Benken Design (BBD). Three biosorption scenarios using the MRS with desirability functions were proposed and implemented. The first biosorption optimization scenario was based on the consumption of raw materials for the process of nickel removal. It sought to minimize the biosorbent dosage consumption (*bioDose*) in order to obtain the highest Ni(II) removal efficiency (*%NiR*). The second biosorption optimization scenario was based on minimizing the energy consumption (minimize stirring speed *S*) to also obtain the highest Ni(II) removal efficiency (*%NiR*). The objective of third optimization scenario was to maximize the efficiency of Ni(II) removal (*%NiR*) for all the values of the established input variable. The experimental results approximated those that the regression models had predicted. This work provides a method that could be applicable to nickel ions reduction from wastewater in a safe, environmentally friendly, and economical way, while solving the problem of accumulation of olive stone waste.

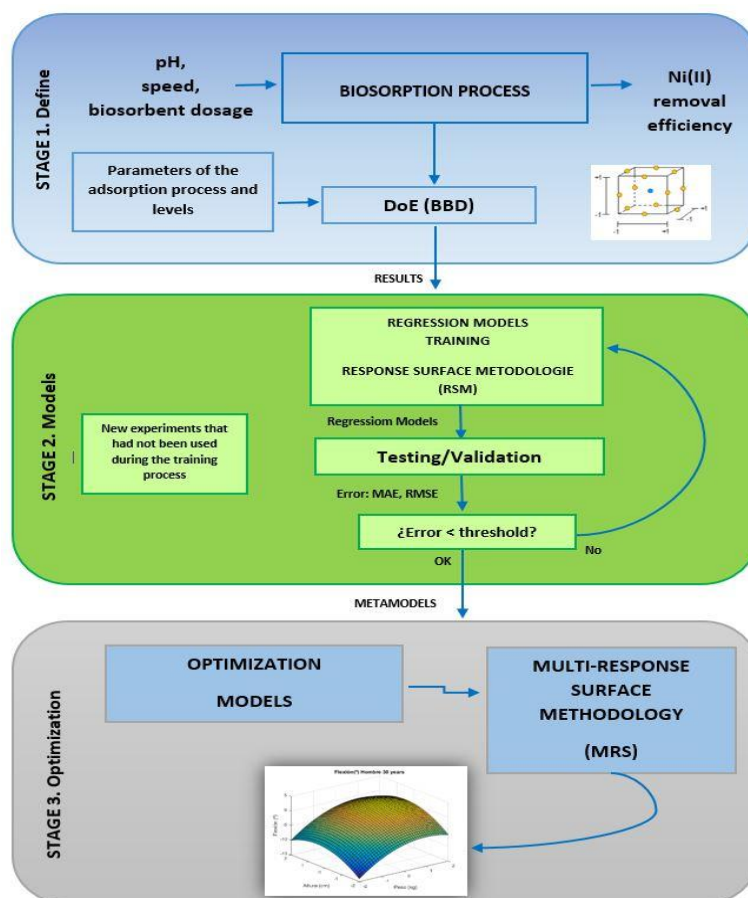


Figure 1. The main stages of the study.

2. Materials and Methods

2.1. Materials

The olive stone waste was provided by an oil extraction plant, called “Trujal 5 Valleys Cooperative Society”, which is located in Arnedo, in the province of La Rioja (Spain). The cultivated olives belonged to the *Olea europaea* species (*Arbequina* variety). The extraction process is carried out in late autumn or early winter. The olive stones were obtained from the separation of the olive pie by an industrial boning machine. The solids were ground by a hammer mill and then dried in an oven at 105 °C. A fraction that consisted of particles of less than 1 mm was chosen as the biosorbent for all of the experiments. The main characteristics of the olive stone waste that was used in the experiments appear in Table 1. Because it was not possible in this study to have “real” industrial water of differing concentrations of nickel, a synthetic effluent or solution that contained Ni(II) was prepared in the laboratory. This solution of nickel (1000 mg/L) was prepared by dissolving 2.475 g of Ni(II) nitrate hexahydrate ($N_2NiO_6 \cdot 6H_2O$) in 500 mL of deionized water. All of the synthetic effluent samples that were required in this study were prepared from this solution with a dilution in deionized water to different nickel concentrations. For pH regulation, hydrochloric acid (HCl) and 0.1 M solutions of sodium hydroxide (NaOH), both of analytical quality, were prepared. The pH adjustment process used a GLP 22 CRISON pH-meter (Crison Instruments SA, Barcelona, Spain), according to the ASTM D1293-18 [49] standard. Only reagents of analytical grade were used (GR for analysis, Merck, Darmstadt, Germany). The effect of biosorbent dose, stirring speed, and solution pH were studied in batch experiments at a fixed initial metal concentration (50 mg/L) and contact time (15 min.) at room temperature.

Table 1. Physicochemical properties of olive stone.

Parameter	Value
Specific surface area (m ² /g)	0.6
Oxygen (%)	41.7
Carbon (% dry weight)	50.7
Nitrogen (% dry weight)	0.4
Sulfur (% dry weight)	0.04
Hydrogen (% dry weight)	5.9
Lignin (g/kg)	387.0
Cellulose (g/kg)	269.0
Hemicellulose (g/kg)	346.0

2.2. Response Surface Method and Design of Experiments

The RSM method is used to determine the relationships of input variables to each other and the output variables. Box and Wilson introduced it in 1951 [50] for experimental data that would be used for optimal responses or for models. Initially, this methodology was created to model the experimental responses. More recently, it has been used for the modeling and optimizing mechanical devices and biomechanical studies from Finite Element Analysis. [51,52]. The RSM method previously always used a Design of Experiments (DoE) [53] with the aim of creating accurate regression models from the least possible amount of data. Several methods have been proposed to develop DoE. However, they generally require the construction of a design matrix (inputs) to measure the outputs or responses of the experiments. One of the most widely used methods is the full factorial design method [54]. This method is based on the adoption of all possible combinations of the values (or levels) and the factors that are considered in the DoE. The use of this method in this study (when considering the three input variables) requires 27 experiments. Central Composite Design (CCD) is another method that is used to develop a DoE. This method is considered to be a fractional three-level design that is useful in obtaining regression models. It requires 16 experiments. However, a Box–Behnken design (BBD) has the advantage of requiring a significantly lower number of experiments [50]. In this study, a Box–Behnken (BBD) with three factors and three levels was chosen for the development of the DoE. It requires 13 experiments to be conducted. Furthermore, four additional experiments with the same variable input as any one of the DoE were conducted in order to determine the repeatability of the experiments. In this case, the input variables for the DoE were speed (*S*), pH (*pH*), and biosorbent dosage (*bioDose*). The optimization factors that were adopted based on experimentation and their ranges were: pH (3.5–6.5), mixing speed (100–200 rpm), and biosorbent dosage (0.5–1.5 g/L) (see Table 2).

Table 2. Adsorption process variables and levels.

Input	Notation	Magnitude	Levels		
			−1	0	1
pH	<i>pH</i>		3.5	5	6.5
Speed	<i>S</i>	rpm	100	150	200
Biosorbent dosage	<i>bioDose</i>	g/L	0.5	1	1.5

After setting the adsorption process variables and levels, as shown in Table 2, R Statistical Software [55] was used to create the design matrix. It was necessary to conduct 17 experiments in order to cover all possible nickel adsorption process input variables and to obtain regression models for use in finding the optimal inputs for the nickel adsorption process. The design matrix (Table 3) indicates the number of experiments and values of the combinations of input variables (pH, speed, and biosorbent dosage) and the process output results of the nickel adsorption process: the removal efficiency of the Ni(II) and the Ni(II) uptake, as determined by Equations (1) and (2), respectively.

Table 3. Design matrix and process output results for the nickel adsorption process.

Sample	Input Variables of the Adsorption Process			Process Outputs	
	pH (pH)	Speed (S) (rpm)	Biosorbent Dosage (<i>bioDose</i>) (g/L)	Ni(II) Removal Efficiency (%NiR) (%)	Ni(II) Uptake (<i>q</i>) (mg/g)
1	3.5	100	1	58.71	29.36
2	6.5	100	1	66.08	33.04
3	5	100	0.5	43.14	43.14
4	5	150	1	53.93	26.97
5	3.5	150	1.5	45.43	15.14
6	5	200	1.5	51.45	17.15
7	3.5	150	0.5	37.7	37.70
8	5	150	1	56.72	28.36
9	5	200	0.5	48.34	48.34
10	6.5	150	1.5	62.43	20.81
11	5	150	1	53.15	26.58
12	6.5	150	0.5	57.24	54.24
13	6.5	200	1	67.28	33.64
14	5	150	1	54.72	27.36
15	5	150	1	53.74	26.87
16	5	100	1.5	59.78	19.93
17	3.5	200	1	49.68	24.84

2.3. Nickel Adsorption Experiments

The experiments were conducted in a laboratory scale setup and in accordance with the Box–Behnken design (BBD) matrix. To each 100 mL solution of 50 mg/L Ni(II) initial concentration (according to Section 2.1) and known pH, a desired quantity of the biosorbent was added in a glass flask. The mixture was stirred on a magnetic hot plate stirrer at room temperature. The stirring speed was differed for each experiment and it was maintained for a predetermined time of 15 min. The process output that was used to select the removal efficiency of nickel was established in each experiment. The biosorbent was separated by filtration with 0.2 µm filters. All of the samples were then added to volumetric flasks and analyzed to determine the residual nickel concentration. The latter was determined by a Unicam-929 atomic adsorption spectrophotometer (Unicam Ltd., Cambridge, UK). Equations (1) and (2) can be used to determine the removal efficiency *E* (%) and metal uptake *q* (mg/g).

$$E (\%) = \frac{(C_I - C_F)}{C_I} \cdot 100 \quad (1)$$

$$q = \frac{(C_I - C_F) \cdot V}{w} \quad (2)$$

where *V* (L) is the volume of the solution, *C_I* and *C_F* (mg/L) are the initial and final concentrations of nickel in the solution, and *w* (g) denotes the amount of biosorbent that was used. The experiments were conducted in duplicate with the average results reported.

3. Results and Discussion

3.1. Experimental Results

The Ni(II) removal efficiency of the process was experimentally determined after determining the input variables of the process of adsorption from the DoE. Table 3 provides the output variables (%NiR and *q*) that were experimentally obtained according to the Box–Behnken DoE design matrix.

3.2. Regression Model Analysis

The data in Table 3 were used to fit Equation (3) to obtain a regression equation for the response by use of the “R” package [55]. Subsequently, second order polynomial models were constructed for the response %NiR. Next, several criteria (p -value, MAE, RMSE, coefficient of determination or R^2 , and adjusted R^2) were used to select the most accurate regression model. The Akaike Information Criterion (AIC) was used in this case to only select the significant terms of the quadratic regression model. This criterion was applied by means of the function “step”, which is available in the “R” package.

$$\begin{aligned} \%NiR = & 63.23261111 + 0.0825105 \cdot bioDose - 2.702 \times 10^{-5} \cdot bioDose^2 - 13.34027778 \cdot pH \\ & + 1.33511111 \cdot pH^2 - 0.42038 \cdot S - 0.0001353 \cdot bioDose \cdot S + 0.0341 \cdot pH \cdot S + 0.0011926 \cdot S^2 \end{aligned} \quad (3)$$

The p -value (or Prob. > F) is the probability that a result will be obtained that equals or exceeds what had been actually observed, if the regression quadratic models are accurate. It can be determined from the analysis of variance (ANOVA). One might consider the model to be acceptable at a confidence interval of $(1 - \alpha)$ if Prob. > F for the quadratic regression model and none of terms of the model are greater than the level of significance (e.g., $\alpha = 0.05$). The Mean Absolute Error (MAE) and the Root Mean Squared Error (RMSE) determine the generalization capacities of the regression models and could be calculated, as follows:

$$MAE = \frac{1}{m} \cdot \sum_{k=1}^m |Y_{k \text{ Experiment}} - Y_{k \text{ Model}}| \quad (4)$$

$$RMSE = \sqrt{\frac{1}{m} \sum_{k=1}^m (Y_{k \text{ Experiment}} - Y_{k \text{ Model}})^2} \quad (5)$$

In this case, $Y_{k \text{ Experiment}}$ are the outputs that were experimentally obtained, whereas $Y_{k \text{ Model}}$ are the outputs of the quadratic models that were produced by RSM and m is the number of experiments. In addition, the coefficient of determination or R^2 indicates the goodness of fit of the regression model, whereas the adjusted R^2 introduces a penalty to the value of R^2 for each predictor (in this case input variable) that is included in the regression model.

Table 4 shows the ANOVA results for the best regression quadratic model obtained and whether the effects or interaction effects are statistically significant (p -value < 0.05). The ANOVA that was undertaken leads one to conclude that $bioDose$ and pH directly influence the Ni(II) remove efficiency (%NiR) (p -value = 0.0005399 and p -value = 6.093×10^{-6} , respectively). In addition, it was noted that, in the ANOVA, S does not have as significant an influence as the other input variables (p -value = 0.0995499). The remaining terms that appear in Equation (3) ($bioDose$; $bioDose^2$; pH^2 ; $bioDose \cdot S$; $pH \cdot S$, and S^2) are input variables that are combined with each other and have a notable influence on %NiR, when considering its statistically significant (p -value < 0.05). In this case, we can conclude that the main effects, square effects, and interaction effects of $bioDose$ and pH were the significant model terms. Therefore, the input variables that were employed for the regression quadratic models can be considered to be statistically significant.

Table 4. ANOVA values for the Ni(II) remove efficiency quadratic model.

Variables	Df	Sum of Sq.	Mean Sq.	F Value	p-Value
<i>bioDose</i>	1	133.4165	133.416	30.8221	0.0005399
<i>bioDose</i> ²	1	174.7524	174.752	40.3717	0.0002197
<i>pH</i>	1	472.9350	472.935	109.2586	6.093 × 10 ⁻⁶
<i>pH</i> ²	1	42.1860	42.1860	9.7459	0.0141890
<i>S</i>	1	15.0152	15.0152	3.4688	0.0995499
<i>bioDose</i> · <i>S</i>	1	45.7652	45.7652	10.5727	0.0116734
<i>pH</i> · <i>S</i>	1	26.1632	26.1632	6.0442	0.0394099
<i>S</i> ²	1	37.4288	37.4288	8.6468	0.0186935
<i>Residuals</i>	8	34.6286	4.32858		

In addition, Table 5 shows the coefficient of determination or R^2 and the adjusted R^2 . It can be seen that the values of both coefficients in this table are very close to 1 ($R^2 = 0.9647$ and adjusted $R^2 = 0.9295$), which is very high. This indicates that there is a high correlation between the observed and predicted values. Additionally, the values corresponding to MAE and RMSE that are shown in this table are very small (MAE = 4.005% and RMSE = 4.825%). This indicates that the adjustment of the regression model is relatively accurate and it has a good generalization capacity.

Table 5. Results of the R^2 , adjusted R^2 , and errors in predicting the Ni(II) remove efficiency when using the quadratic regression model that is obtained.

R^2	Adjusted R^2	MAE Train	RMSE Train
0.9647	0.9295	0.04005	0.04825

Five new experiments were conducted during the training process to test the regression models. Table 6 illustrates this matrix for the Ni(II) biosorption process.

Table 6. Test matrix of the Ni(II) biosorption process.

Sample	Input Variables of the Adsorption Process			Process Outputs	
	pH (<i>pH</i>)	Speed (<i>S</i>) (rpm)	Biosorbent Dosage (<i>bioDose</i>) (g/L)	Ni(II) Removal Efficiency (% <i>NiR</i>) (%)	Ni(II) Uptake (<i>q</i>) (mg/g)
1	6.4	174	1.284	65.70	25.58
2	4.6	171	0.956	50.63	26.47
3	6.23	106	0.547	50.07	45.72
4	4.3	199	0.533	45.43	42.64
5	5.5	159	0.526	47.16	44.79

After completing the five new experiments, errors became apparent during the testing stage. Table 7 suggests that the regression models are accurately adjusted to the experimental results (MAE = 5.625% and RMSE = 6.727%).

Table 7. The results of the errors in predicting the Ni(II) remove efficiency using the second order regression models.

MAE Test	RMSE Test
0.05625	0.06727

A scatter diagram was created of the output variable after identifying the errors in prediction of the training and testing data by the regression models (See Figure 2). The blue points indicate the 17

data point values from design matrix for nickel adsorption (Table 3). The red points concern the five additional experiments, as well as that the regression models that were used (Table 6). The closer the points are on the diagonal line, the greater the correlation of the regression models. In this case, both the red points (testing data) and the blue points (training data) are very close to the diagonal line.

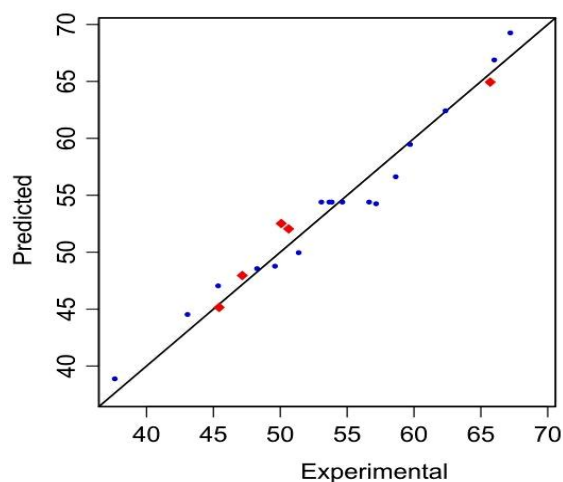


Figure 2. Scatter diagram of Ni(II) removal efficiency.

3.3. Effect of Operational Parameters

3.3.1. Effect of Solution pH on Ni(II) Adsorption

pH is the parameter that most affects the metal ions solubility, the counterion concentration on the functional groups of the biosorbent, and the degree of ionization of the biosorbent during the reaction [38,48]. In this study, the effect of hydrogen ion concentration was investigated in solutions at differing values of pH within a range of 3.5 to 6.5.

Figure 3a,b, respectively, show the effect of the pH of the solution on Ni(II) biosorption at various stirring speeds S (100 150 and 200 rpm) and for different biosorbent dosages $bioDose$ (0.5 and 1.5 g/L). It can be seen in both figures that, if the pH values decrease, the Ni(II) removal efficiency $\%NiR$ also decreases. Additionally, it can be seen in both figures that, at a low adsorbent dose ($bioDose = 0.5$ g/L) and high stirring speed ($S = 200$ rpm), the maximum value of Ni(II) removal efficiency $\%NiR$ is reached when the $pH = 6.5$ (Figure 3a). In contrast, the maximum value of Ni(II) removal efficiency $\%NiR$ is reached at high adsorbent doses ($bioDose = 1.5$ g/L) and a much lower stirring speed ($S = 100$ rpm) when the $pH = 6.5$ (Figure 3b). It can be concluded that what happens is the following: at low pH values, concentrations of H^+ ions greatly exceed that of metal ions. H^+ ions will then compete with Ni(II) ions for the adsorbent surface. This will make it more difficult for the Ni(II) ions to reach the adsorbent binding sites that are caused by repulsive forces. However, the metal removal is minimal. This is thought to be due to greater competition by protons and nickel ions for the binding sites and complex formations. The Ni(II) ions are precipitated when the pH is increased. This is due to the formation of nickel hydroxide precipitates by hydroxide anions [56].

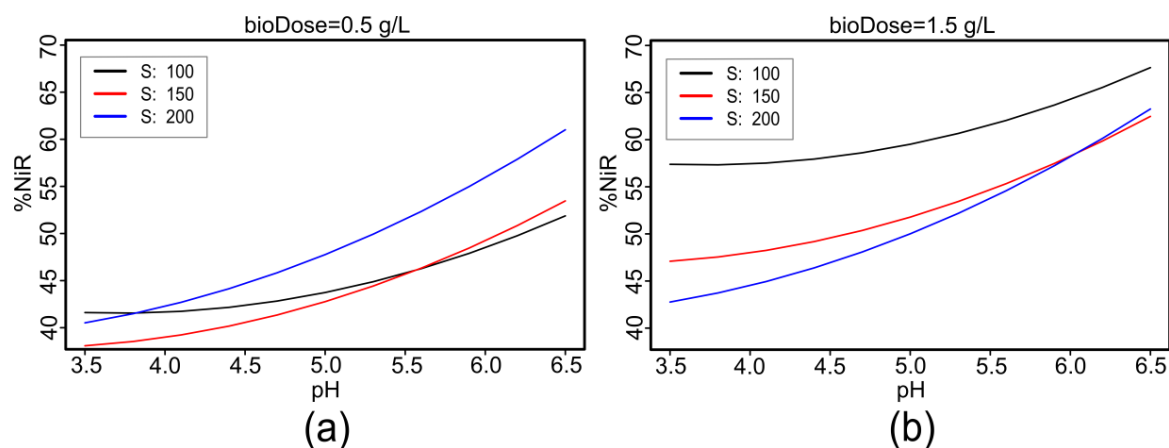


Figure 3. Variation of %NiR vs pH for different values of S when: (a) $bioDose = 0.5$ g/L; (b) $bioDose = 1.5$ g/L.

3.3.2. Effect of Adsorbent Dose on Ni(II) Adsorption

An increase in the biosorption percentage and the biosorbent dose might be due to an increase in availability of sorption sites on the surface of the sorbent [57]. In this study, nickel removal at different adsorbent doses was studied for values of the pH that ranged from 3.5 to 6.5 and with various amounts of adsorbent $bioDose$ of 0.55 to 1.5 g/L when the stirring speed S was a minimum and a maximum (Figure 4a with $S = 100$ rpm and Figure 4b with $S = 200$ rpm, respectively). It is observed in both figures that, as the adsorbent $bioDose$ increases, the nickel removal also increases, as does the pH. This is due to the availability of more and more adsorption sites for complexation of Ni(II) ions [56,58]. However, these figures also indicate that the biosorption percentage has a maximum value, if the adsorbent amount $bioDose$ has a maximum value. For example, in Figure 4a, a maximum value of 69% is observed for the biosorption percentage when the $bioDose$ is 1272.72 rpm (a low stirring speed S), whereas, in Figure 4b, a maximum value of 69.33% is observed for the biosorption percentage when the $bioDose$ is 1027.273 rpm (a high stirring speed S). These maximum values that are found for the biosorption percentage when the amount $bioDose$ values are not the maximum suggest a saturation effect that causes a decrease in the removal of nickel as the $bioDose$ increases.

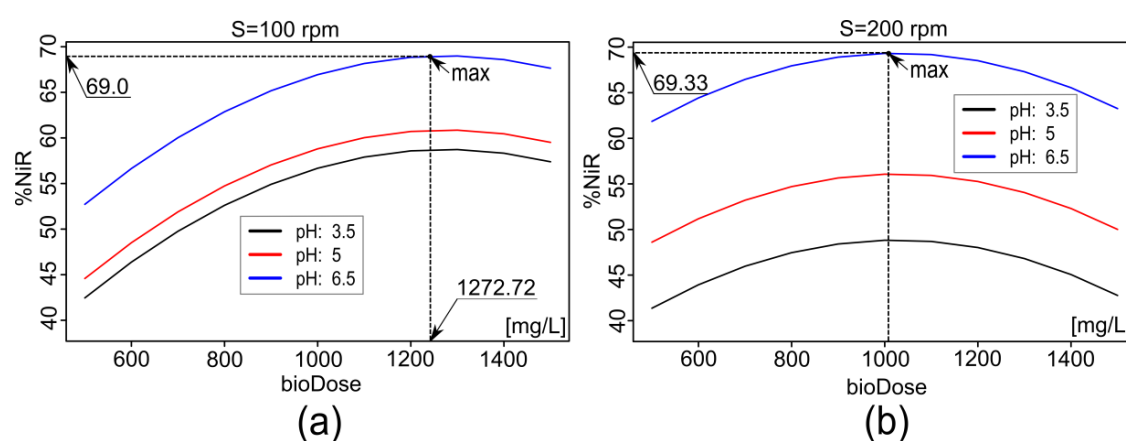


Figure 4. %NiR vs. $bioDose$ for different values of pH when: (a) $S = 100$ rpm; and, (b) $S = 200$ rpm.

3.3.3. Effect of Stirring Speed Dose on Ni(II) Adsorption

Pore diffusion and film control the adsorption rate, depending on the stirring speed. As a general rule, a low stirring speed produces a thicker layer of film of the solvent around the adsorbent. This results in the layer of film controlling the rate of adsorption. A higher stirring speed causes

the thickness of the layer of film around the sorbent to become thinner [38]. Thus, the metal ions move through the film layer very quickly. This leaves diffusion through the pores as the factor that controls the rate of adsorption. However, when the amount of biosorbent dosage increases, this effect does not occur as clearly. How stirring speed affects the percentage adsorption of Ni(II) ions was also investigated. In this case, the stirring speed varied from 100 to 200 rpm for different values of pH (a range of 3.5 to 6.5) and at different values of *bioDose*, as shown in Figure 5. It is seen in Figure 5a that, for low biosorbent dosage values (*bioDose* = 0.5 g/L), the percentage adsorption of Ni(II) values increases as *S* increases. In contrast, Figure 5b shows that, for high values of biosorbent dosage (*bioDose* = 1.5 g/L), the percentage of adsorption of Ni(II) decrease as *S* increases. This effect in the decrease of the percentage adsorption of Ni(II) can be seen, for the point analyzed above, as a saturation effect on the surface of the biosorbent, which is unable to adsorb more Ni(II).

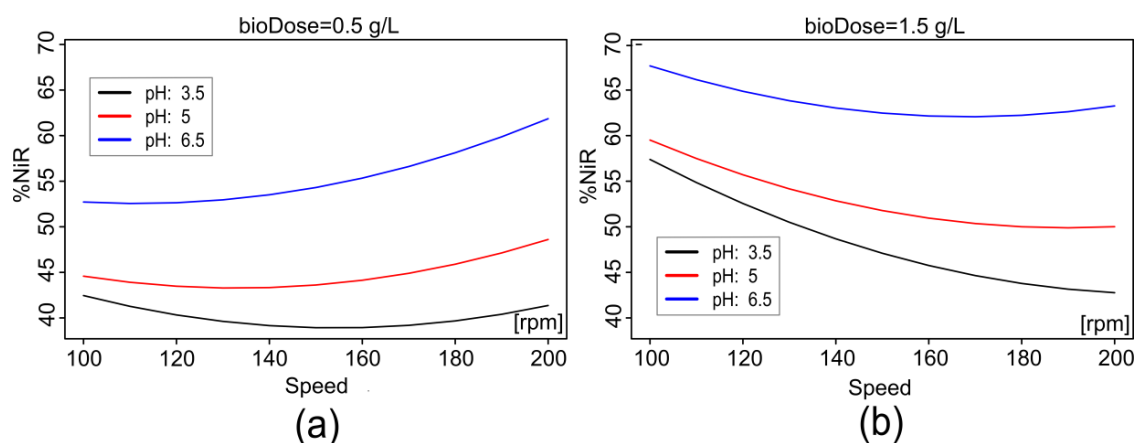


Figure 5. %NiR vs. *S* for different values of *pH* when: (a) *bioDose* = 0.5 g/L; and, (b) *bioDose* = 1.5 g/L.

3.4. Multi-Response Optimization

Tables 8–10 provide the combination of the input variables of adsorption and Ni(II) removal efficiency for the process that was examined when studying, by desirability function, the biosorption of nickel on olive stone waste in wastewater. This involved the desirability package [59] for three criteria or scenarios of biosorption optimization. The first column of each table contains the input variables that were examined, as well as the outputs. The second column indicates the objective for the biosorption optimization process. The third and fourth columns show the minimum and maximum values (range) that have been established for the biosorption adsorption process input variables. Finally, the fifth column provides the optimized values and the sixth column shows the desirability values.

Table 8 provides the results of the first biosorption optimization scenario. Its optimization requirements are based on minimizing the amount of biosorbent that is necessary for obtaining the highest efficiency in removing nickel (maximizing the %NiR). *S* and *pH* input variables are in a range, whereas the *bioDose* is the minimum (0.553 g/L). Additionally, in Table 8, the *pH* value is high (6.369) and *S* is high (199.2 rpm). In this first scenario, the overall desirability was 0.877. Table 9 shows the results of the second biosorption optimization scenario. Its optimization requirements are based on minimizing the biosorption process energy requirements, while obtaining the highest Ni(II) removal efficiency. The *bioDose* and *pH* input variables are in range, and *S* is minimum. In addition, it can be seen in this table that the *pH* value is high (6.43) and that the *bioDose* is also high (1.311 g/L), whereas the stirring speed is a minimum (102 rpm). The overall desirability value of this second scenario was 0.989. Finally, Table 10 shows the results of the third biosorption optimization scenario. In this case, the optimization requirements are based on maximizing %NiR, whereas the input variables are in the range. In addition, Table 10 shows that the *pH* is high (6.43), the *S* is low (102 rpm), and the *bioDose* is high (1.311 g). This indicates that, with an increase in *pH*, the removal efficiency of nickel

will increase when the biosorbent dose is increased. Finally, an overall desirability of 1 was obtained for this third scenario.

Additionally, the results presented in Tables 8–10 show that the output of the studied process regarding (%NiR) is similar to those of all biosorption optimization scenarios in the range of variables for the biosorption process being considered. For instance, the range of the optimal values of the *bioDose* for the three scenarios studied extends from 0.553 to 1.311. In addition, the range of values for the *NiR* percentage extends from 61.732 to 68.158. These results suggest that the optimal variables for the biosorption optimization scenarios appear in a somewhat narrow range, especially for the second and third scenarios.

Table 8. The first biosorption optimization scenario: minimizing the biosorbent dosage consumption to obtain the highest Ni(II) removal efficiency.

Variables	Goal	Min	Max	Optimum	Desirability
<i>bioDose</i>	Min	0.5	1.5	0.553	0.947
<i>pH</i>	inRange	3.5	6.5	6.369	1
<i>S</i>	inRange	100	200	199.234	1
% <i>NiR</i>	Max	37.7	67.28	61.732	0.812
Overall Desirability					0.877

Table 9. The second biosorption optimization scenario: minimizing the energy consumption (minimizing stirring speed) to obtain the highest Ni(II) removal efficiency.

Variables	Goal	Min	Max	Optimum	Desirability
<i>bioDose</i>	inRange	0.5	1.5	1.311	1
<i>pH</i>	inRange	3.5	6.5	6.433	1
<i>S</i>	Min	100	200	102.115	0.979
% <i>NiR</i>	Max	37.7	67.28	68.185	1
Overall Desirability					0.989

Table 10. The third biosorption optimization scenario: maximizing the Ni(II) removal efficiency.

Variables	Goal	Min	Max	Optimum	Desirability
<i>bioDose</i>	inRange	0.5	1.5	1.311	1
<i>pH</i>	inRange	3.5	6.5	6.433	1
<i>S</i>	inRange	100	200	102.315	1
% <i>NiR</i>	Max	37.7	67.28	68.158	1
Overall Desirability					1

Figure 6a shows, in three dimensions, the results of the first biosorption optimization scenario in order to graphically check the optimal scenarios that have been obtained. These include the variation in Ni(II) removal efficiency (%*NiR*) when the *pH* is 6.369 and the other input variables are in range (*S* (100–200) and *bioDose* (0.5–1.5)). However, Figure 6b shows it graphically, and in two dimensions (the horizontal axis corresponds to *S* and the vertical axis corresponds to *bioDose*) the variation of %*NiR* for the same 6.369 *pH* value). It can be deduced from both figures that the parameter *S* for this the first biosorption optimization scenario is practically at the upper end of the interval (199.234) and the %*NiR* could reach much higher values than those achieved in this first biosorption optimization scenario.

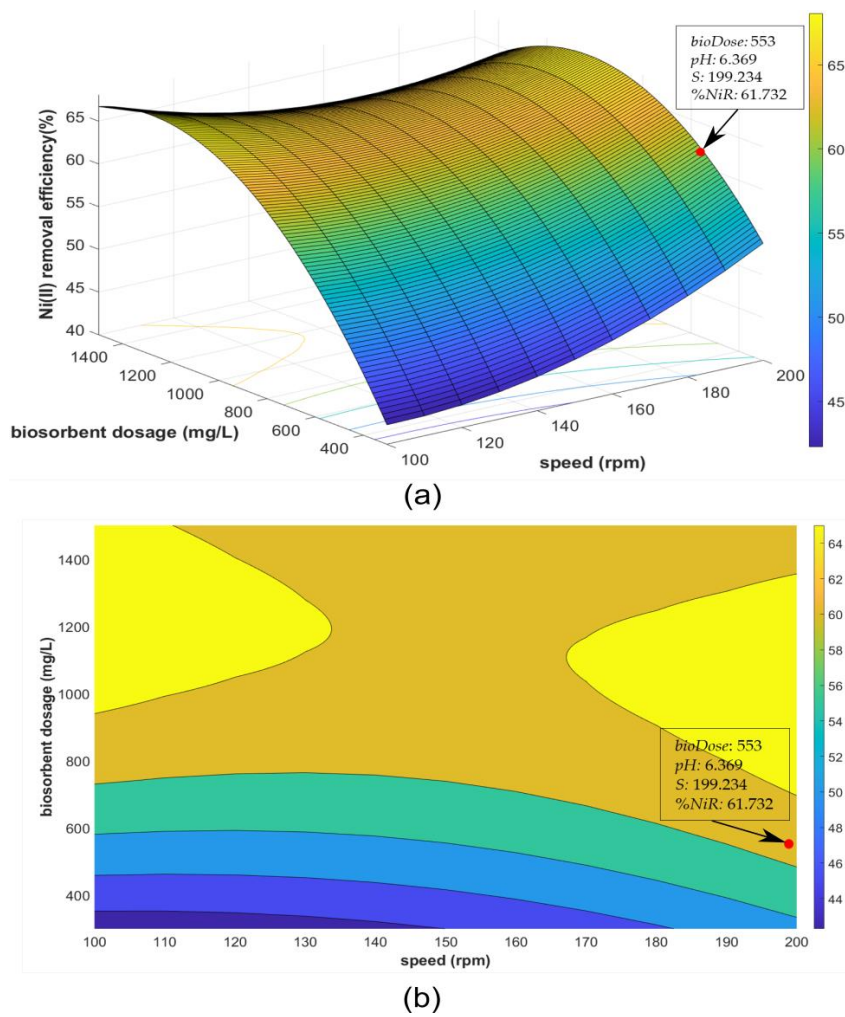


Figure 6. First optimization scenario: (a) response surface plot showing the effect of *S* and *bioDose*, (b) contour plot showing the optimal point reached.

Figure 7a shows in three dimensions the results that were achieved for the second and third biosorption optimization scenarios. The results show the variation in Ni(II) removal efficiency (%NiR) when the *pH* is 6.433 and the other input variables are in range (*S* (100–200) and *bioDose* (0.5–1.5)). As this figure shows, the optimal points are very close together (See Tables 8 and 9) and difficult to differentiate. The range of the input variables *S* (101–103) and *bioDose* (1312–1312) has been reduced in Figure 7b, while maintaining the *pH* value of 6.433, in order to appreciate these two optimal points. This figure shows that the optimal variables for the second and for the third biosorption optimization scenarios appear in a narrow range.

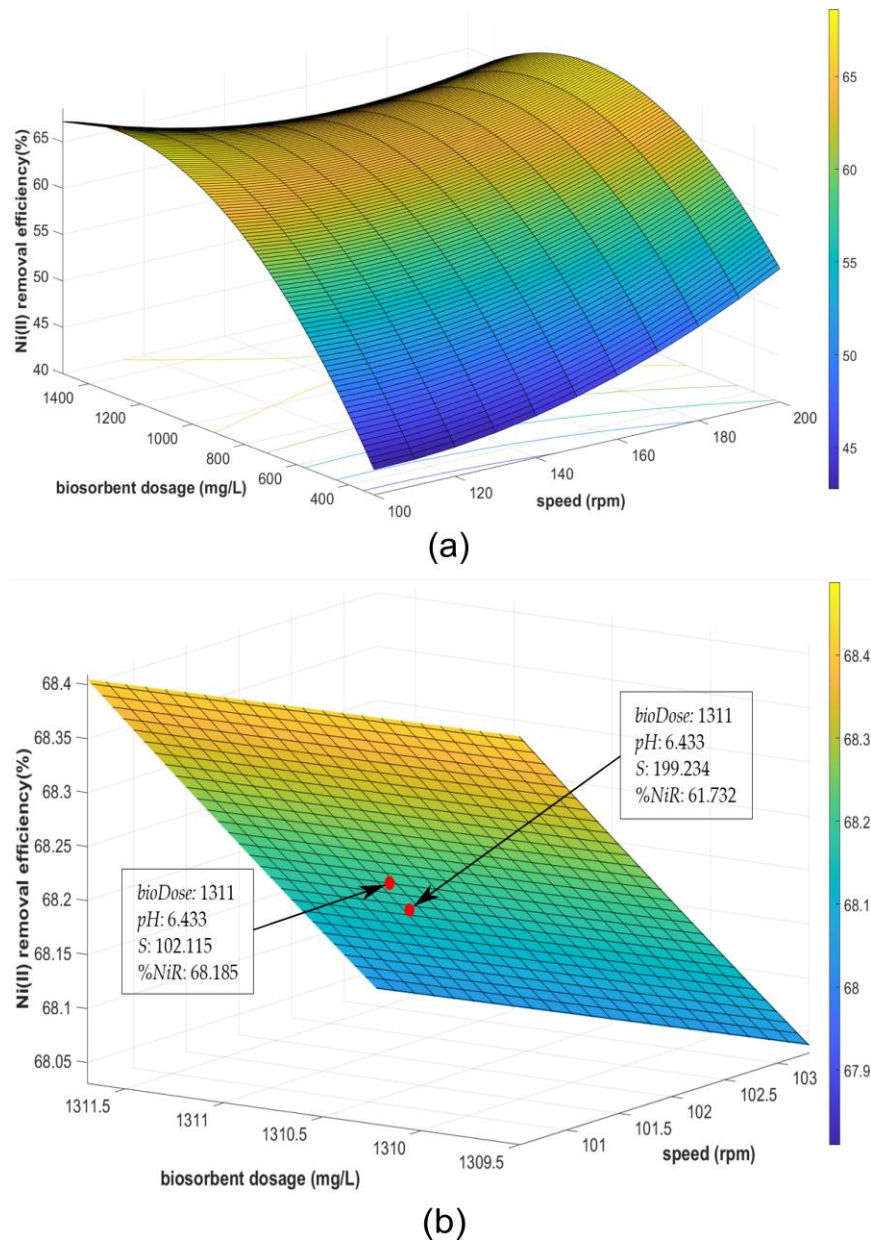


Figure 7. Second and third optimization scenario: (a) response surface plot showing the effect of *S* and *bioDose*, (b) detail the optimal points reached.

Table 11 shows the maximum adsorption capacity (q) for the three optimization scenarios that have been calculated according Equation (2) with the input variables that appear in Tables 8–10. This table shows that the maximum values for q are reached in the first optimization scenario ($q = 55.816$ mg/g). That scenario consists of minimizing the biosorbent dosage consumption to obtain the highest Ni(II) removal efficiency. The second and third optimization scenarios show $\%NiR$ values that are higher than in the first optimization scenario (26.005 mg/g and 25.995 mg/g, respectively). However, they show higher *bioDose* values (1.311 g/L for both scenarios). This difference between the values that were obtained for $\%NiR$ and *bioDose* gives rise to a greatly different q for the first scenario.

Table 11. Adsorption capacity of the olive stone waste.

Opt. Scenario	pH	S (rpm)	bioDose (g/L)	%NiR (%)	q (mg/g)
1st Scenario	6.369	199.234	0.553	61.732	55.816
2nd Scenario	6.433	102.115	1.311	68.185	26.005
3rd Scenario	6.433	102.315	1.311	68.158	25.995

Three new experiments were conducted after obtaining the input variables of the three biosorption optimization scenarios. They employed the process variable combinations that appear in Tables 8–10 to test the accuracy of the proposed method. Table 12 provides the output variable values of the three studied biosorption optimization scenarios that were experimentally obtained ($\%NiR_{Exp.}$). This table also shows the MAE and RMSE values, the experimentally determined ($\%NiR_{Exp.}$), and from the data in Table 11. The last column contains errors that concern the MAE for the values of output variable ($\%NiR$) in each clarification optimization scenario. The MAE and RMSE in the last two rows relate to the errors in output variable values of the clarification optimization scenarios that were examined. The table shows that there was a very small difference between values that were experimentally obtained for the three biosorption optimization scenarios and those that the RSM methodology produced (see the the results in Tables 8–10). Additionally, this table shows that the first optimization scenario has the lowest MAE (0.034), whereas the second has the highest (0.379), and the MAE for the third scenario is 0.038.

Table 12. Experimental output variable ($\%NiR_{Exp.}$) of the three biosorption optimization scenarios and errors calculated.

Opt. Scenario	Exp. Values	Errors
	$\%NiR_{Exp.}$	MAE
1st Scenario	61.697	0.034
2nd Scenario	68.564	0.379
3rd Scenario	68.223	0.038
MAE	0.1504	
RMSE	0.2209	

3.5. SEM-EDX Analysis

The samples were analyzed by atomic absorption spectroscopy to ensure that the olive stone waste that had been used as a biosorbent retained nickel. Scanning Electron Microscopy with Energy Dispersive X-ray spectroscopy (SEM-EDX) also was employed to identify any nickel in olive stone waste. In this case, a sample of the olive stone waste not used as an adsorbent (raw) and another sample of waste that was used as an adsorbent (the one used in the second optimization scenario) were compared. The reason for analyzing the adsorbent that was employed in the second optimization scenario using SEM is that this scenario had a higher $\%NiR$ in the removal of nickel (68.185%) than the others (61.732% and 68.158%). Figure 8a shows the olive stone waste before and after Figure 8b metal biosorption SEM micrographs. Figure 8b shows that there is nickel trapped in the olive stone waste. This indicates that this type of organic waste can be used as an adsorbent for the removal of nickel.

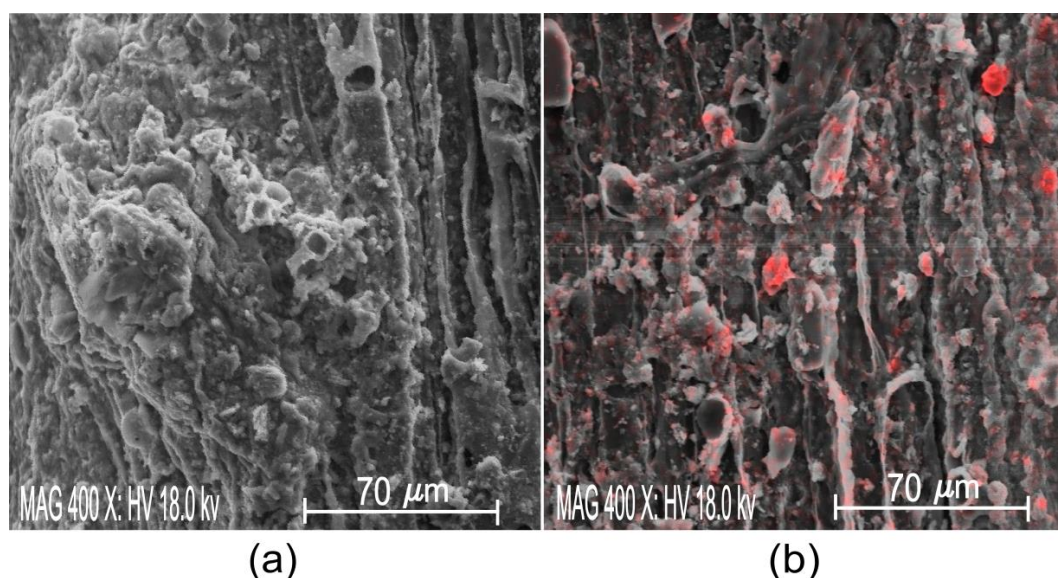


Figure 8. Olive stone waste surface morphology as recorded by scanning electron microscopy: (a) before metal-ion biosorption, (b) after Ni(II) biosorption. Visible nickel appears in red.

4. Conclusions

Determining the amount of biosorbent that is necessary for the removal of nickel ions from wastewater is a complicated task. This paper provides a methodology that is based on RSM with desirability functions to optimize the biosorption process for efficient removal of Ni(II) from wastewater sample while using olive stone waste as a cheap biosorbent. The proposed methodology generates a quadratic regression model from a DoE. The output variable Ni(II) removal efficiency ($\%NiR$) is a function of the input variables biosorbent dosage ($bioDose$), pH , and stirring speed (S). After the regression model is validated, multi-objective optimization is conducted when considering three biosorption optimization scenarios and using desirability functions. These are the biosorbent dosage consumption, energy consumption, and Ni(II) removal efficiency. In the results of the optimization study, the pH reached an optimum value in a range from 6.369 to 6.433, a stirring speed (S) of 102.115 rpm to 199.234 rpm, and a biosorbent dosage ($bioDose$) of 0.553 g/L to 1.311 g/L. The foregoing suggests that optimal biosorption inputs variables can be found when various biosorption optimization scenarios are satisfied in a relatively narrow range. Finally, the three biosorption scenarios were verified in order to test the accuracy of the proposed methodology. The values that were obtained for $\%NiR$ from the optimization based on RSM were 61,732%, 68,185%, and 68,158% for each of the optimization scenarios. However, the experimental results obtained for $\%NiR_{Exp.}$ in each of the optimization scenarios showed that the values were very similar to those that were theoretically obtained (61.697%, 68.564%, and 68.223%). It was concluded that there was good agreement between the experimental results and the predicted results. In conclusion, this paper has shown that the proposed methodology might be an efficient means for the removal of nickel ions from wastewater in a safe, environmentally friendly, and economical way, while solving the problem of the accumulation of olive stone waste.

Author Contributions: Experimental Work: M.C.B., R.L.L. and F.S.G.; Contributions to development of predictive models and optimization: R.E.G.; Results analysis, revision and improvement of the manuscript: M.C.B., R.L.L., R.E.G. and F.S.G. All authors have read and agreed to the published version of the manuscript.

Funding: This research received no external funding.

Acknowledgments: The authors wish to thank the La Rioja Government as well as to the Institute of Riojan Studies (IER) for funding part of this research.

Conflicts of Interest: The authors declare no conflict of interest.

References

1. Directive 2010/75/EU of the European Parliament and of the council of 24 November 2010 on industrial emissions. *Off. J. Eur. Union* **2010**, *334*, 17–119.
2. Raval, N.P.; Shah, P.U.; Shah, N.K. Adsorptive removal of nickel (II) ions from aqueous environment: A review. *J. Environ. Manag.* **2016**, *179*, 1–20. [[CrossRef](#)] [[PubMed](#)]
3. Dabrowski, A.; Hubicki, Z.; Podkoscielny, P.; Robens, E. Selective removal of the heavy metal ions from waters and industrial wastewaters by ion-exchange method. *Chemosphere* **2004**, *56*, 91–106. [[CrossRef](#)] [[PubMed](#)]
4. Shaidan, N.H.; Eldemerdash, U.; Awad, S. Removal of Ni (II) ions from aqueous solutions using fixed-bed ion exchange column technique. *J. Taiwan Inst. Chem. Eng.* **2012**, *43*, 40–45. [[CrossRef](#)]
5. Dermentzis, K.; Christoforidis, A.; Valsamidou, E.; Loucas, A. Removal of nickel, copper, zinc and chromium from synthetic and industrial wastewater by electrocoagulation. *Int. J. Environ. Sci.* **2011**, *1*, 697–710.
6. Heidmann, I.; Calmano, W. Removal of Zn (II), Cu (II), Ni (II), Ag (I) and Cr (VI) present in aqueous solutions by aluminium electrocoagulation. *J. Hazard. Mater.* **2008**, *152*, 934–941. [[CrossRef](#)]
7. Samper, E.; Rodríguez, M.; De la Rubia, M.A.; Prats, D. Removal of metal ions at low concentration by micellar-enhanced ultrafiltration (MEUF) using sodium dodecyl sulfate (SDS) and linear alkylbenzene sulfonate (LAS). *Sep. Purif. Technol.* **2009**, *65*, 337–342. [[CrossRef](#)]
8. Molinari, R.; Poerio, T.; Argurio, P. Selective separation of copper (II) and nickel (II) from aqueous media using the complexation-ultrafiltration process. *Chemosphere* **2008**, *70*, 341–348. [[CrossRef](#)]
9. Siboni, M.S.; Samadi, M.T.; Yang, J.K.; Lee, S.M. Photocatalytic reduction of Cr (VI) and Ni (II) in aqueous solution by synthesized nanoparticle ZnO under ultraviolet light irradiation: a kinetic study. *Environ. Technol.* **2011**, *32*, 1573–1579. [[CrossRef](#)]
10. Ipek, U. Removal of Ni (II) and Zn (II) from an aqueous solution by reverse osmosis. *Desalination* **2005**, *174*, 161–169. [[CrossRef](#)]
11. Mohsen-Nia, M.; Montazeri, P.; Modarress, H. Removal of Cu²⁺ and Ni²⁺ from wastewater with a chelating agent and reverse osmosis processes. *Desalination* **2007**, *217*, 276–281. [[CrossRef](#)]
12. Belkacem, M.; Khodir, M.; Abdelkrim, S. Treatment characteristics of textile wastewater and removal of heavy metals using the electroflotation technique. *Desalination* **2008**, *228*, 245–254. [[CrossRef](#)]
13. Saeed, A.; Iqbal, M.; Akhtar, M.W. Removal and recovery of lead (II) from single and multimetal (Cd, Cu, Ni, Zn) solutions by crop milling waste (black gram husk). *J. Hazard. Mater.* **2005**, *117*, 65–73. [[CrossRef](#)] [[PubMed](#)]
14. Do, Q.C.; Choi, S.; Kim, H.; Kang, S. Adsorption of lead and nickel on to expanded graphite decorated with manganese oxide nanoparticles. *Appl. Sci.* **2019**, *9*, 5375. [[CrossRef](#)]
15. Manjuladevi, M.; Anitha, R.; Manonmani, S. Kinetic study on adsorption of Cr (VI), Ni (II), Cd (II) and Pb (II) ions from aqueous solutions using activated carbon prepared from *Cucumis melo* peel. *Appl. Water Sci.* **2018**, *8*, 1–36. [[CrossRef](#)]
16. Afroz, S.; Sen, T.K. A review on heavy metal ions and dye adsorption from water by agricultural solid waste adsorbents. *Water Air Soil Pollut.* **2018**, *229*, 225. [[CrossRef](#)]
17. Basu, M.; Guha, A.K.; Ray, L. Adsorption of lead on cucumber peel. *J. Clean. Prod.* **2017**, *151*, 603–615. [[CrossRef](#)]
18. Şen, A.; Pereira, H.; Olivella, M.A.; Villaescusa, I. Heavy metals removal in aqueous environments using bark as a biosorbent. *Int. J. Environ. Sci. Technol.* **2015**, *12*, 391–404. [[CrossRef](#)]
19. Gupta, V.K.; Mittal, A.; Malviya, A.; Mittal, J. Adsorption of carmoisine A from wastewater using waste materials-bottom ash and deoiled soya. *J. Colloid Interface Sci.* **2009**, *335*, 24–33. [[CrossRef](#)]
20. Tunalı, S.; Akar, T. Zn (II) biosorption properties of *Botrytis cinerea* biomass. *J. Hazard. Mater.* **2006**, *131*, 137–145. [[CrossRef](#)]
21. Beolchini, F.; Pagnanelli, F.; Toro, L.; Veglio, F. Ionic strength effect on copper biosorption by *Sphaerotilus natans*: Equilibrium study and dynamic modelling in membrane reactor. *Water Res.* **2006**, *40*, 144–152. [[CrossRef](#)] [[PubMed](#)]
22. Qi, B.C.; Aldrich, C. Biosorption of heavy metals from aqueous solutions with tobacco dust. *Bioresour. Technol.* **2008**, *99*, 5595–5601. [[CrossRef](#)] [[PubMed](#)]

23. Pahlavanzadeh, H.; Keshtkar, A.R.; Safdari, J.; Abadi, Z. Biosorption of nickel (II) from aqueous solution by brown algae: equilibrium, dynamic and thermodynamic studies. *J. Hazard. Mater.* **2010**, *175*, 304–310. [[CrossRef](#)] [[PubMed](#)]
24. Fiol, N.; Escudero, C.; Villaescusa, I. Re-use of exhausted ground coffee waste for Cr (VI) sorption. *Sep. Sci. Technol.* **2008**, *43*, 582–596. [[CrossRef](#)]
25. Iqbal, M.; Schiewer, S.; Cameron, R. Mechanistic elucidation and evaluation of biosorption of metal ions by grapefruit peel using FTIR spectroscopy, kinetics and isotherms modeling, cations displacement and EDX analysis. *J. Chem. Technol. Biotechnol.* **2009**, *84*, 1516–1526. [[CrossRef](#)]
26. Mata, Y.N.; Blázquez, M.L.; Ballester, A.; González, F.; Muñoz, J.A. Optimization of the continuous biosorption of copper with sugar-beet pectin gels. *J. Environ. Manage.* **2009**, *90*, 1737–1743. [[CrossRef](#)]
27. Villaescusa, I.; Fiol, N.; Martínez, M.; Miralles, N.; Poch, J.; Serarols, J. Removal of copper and nickel ions from aqueous solutions by grape stalks wastes. *Water Res.* **2004**, *38*, 992–1002. [[CrossRef](#)]
28. Wu, Y.; Fan, Y.; Zhang, M.; Ming, M.; Yang, S.; Arkin, A. Functionalized agricultural biomass as a low-cost adsorbent : Utilization of rice straw incorporated with amine groups for the adsorption of Cr (VI) and Ni (II) from single and binary systems. *Biochem. Eng. J.* **2016**, *105*, 27–35. [[CrossRef](#)]
29. Razafsha, A.; Ziarati, P.; Moslehishad, M. Removal of heavy metals from oryza sativa rice by sour lemon peel as bio-sorbent. *Biomed. Pharmacol. J.* **2016**, *9*, 543–553. [[CrossRef](#)]
30. Sudha, R.; Srinivasan, K.; Premkumar, P. Kinetic, mechanism and equilibrium studies on removal of Pb (II) using Citrus limettioides peel and seed carbon. *Res. Chem. Intermed.* **2016**, *42*, 1677–1697. [[CrossRef](#)]
31. Lam, Y.F.; Yee, L.; Chua, S.J.; Lim, S.S.; Gan, S. Ecotoxicology and environmental safety insights into the equilibrium, kinetic and thermodynamics of nickel removal by environmental friendly *Lansium domesticum* peel biosorbent. *Ecotoxicol. Environ. Saf.* **2016**, *127*, 61–70. [[CrossRef](#)] [[PubMed](#)]
32. Argun, M.E.; Dursun, S.; Gur, K.; Ozdemir, C.; Karatas, M.; Dogan, S. Nickel adsorption on the modified pine tree materials. *Environ. Technol.* **2005**, *26*, 479–488. [[CrossRef](#)] [[PubMed](#)]
33. Kumar, P.S.; Ramalingam, S.; Kirupha, S.D.; Murugesan, A.; Vidhyadevi, T.; Sivanesan, S. Adsorption behavior of nickel (II) onto cashew nut shell: equilibrium, thermodynamics, kinetics, mechanism and process design. *Chem. Eng. J.* **2011**, *167*, 122–131. [[CrossRef](#)]
34. Bobadilla, C.M.; González Marcos, A.; Vergara González, E.P.; Alba-Elías, F. Bioremediation of waste water to remove heavy metals using the spent mushroom substrate of *Agaricus bisporus*. *Water* **2019**, *11*, 454. [[CrossRef](#)]
35. Flores-Garnica, J.G.; Morales-Barrera, L.; Pineda-Camacho, G.; Cristiani-Urbina, E. Biosorption of Ni (II) from aqueous solutions by Litchi chinensis seeds. *Bioresour. Technol.* **2013**, *136*, 635–643. [[CrossRef](#)] [[PubMed](#)]
36. Bhatnagar, A.; Kaczala, F.; Hogland, W.; Marques, M.; Paraskeva, C.A.; Papadakis, V.G.; Sillanpää, M. Valorization of solid waste products from the olive oil industry as potential adsorbents for water pollution control—A review. *Environ. Sci. Pollut. Res. Int.* **2013**, *21*, 268–298. [[CrossRef](#)]
37. Uğurlu, M.; Kula, I.; Karaoğlu, M.H.; Arslan, Y. Removal of Ni (II) ions from aqueous solutions using activated-carbon prepared from olive stone by ZnCl₂ activation. *Environ. Prog. Sustain. Energy.* **2009**, *28*, 547–557. [[CrossRef](#)]
38. Nuhoglu, Y.; Malkoc, E. Thermodynamic and kinetic studies of environmentally friendly Ni(II) biosorption using waste pomace of an olive oil factory. *Bioresour. Technol.* **2009**, *100*, 2375–2380. [[CrossRef](#)]
39. Fiol, N.; Villaescusa, I.; Martínez, M.; Miralles, N.; Poch, J.; Serarols, J. Sorption of Pb (II), Ni (II), Cu (II) and Cd (II) from aqueous solution by olive stone waste. *Sep. Purif. Technol.* **2006**, *50*, 132–140. [[CrossRef](#)]
40. Blázquez, G.; Hernáinz, F.; Calero, M.; Ruiz-Núñez, L.F. Removal of cadmium ions with olive stones: the effect of some parameters. *Process. Biochem.* **2005**, *40*, 2649–2654. [[CrossRef](#)]
41. Belalia, M.; Bendjelloul, M.; Aziz, A.; Elandaloussi, E.H. Surface modification of olive stone waste for enhanced sorption properties of cadmium and lead ions. *Acta Chem. Iasi* **2018**, *26*, 281–306. [[CrossRef](#)]
42. Witek-Krowiak, A.; Chojnacka, K.; Podstawczyk, D.; Dawiec, A.; Pokomeda, K. Application of response surface methodology and artificial neural network methods in modelling and optimization of biosorption process. *Bioresour. Technol.* **2014**, *160*, 150–160. [[CrossRef](#)] [[PubMed](#)]
43. Garg, U.K.; Kaur, M.P.; Garg, V.K.; Sud, D. Removal of nickel (II) from an aqueous solution by adsorption by agricultural waste biomass using a response surface methodological approach. *Bioresour. Technol.* **2008**, *99*, 1325–1331. [[CrossRef](#)] [[PubMed](#)]

44. Amini, M.; Younesi, H. Biosorption of Cd (II), Ni (II) and Pb (II) from an aqueous solution of dried biomass of *Aspergillus niger*: Application of response surface methodology to the optimization of process parameters. *Clean Soil Air Water* **2009**, *37*, 776–786. [CrossRef]
45. Murugesan, S.; Rajiv, S.; Thanapalan, M. Optimization of process variables for biosorption of nickel (II) using the response surface method. *Korean J. Chem. Eng.* **2009**, *26*, 364. [CrossRef]
46. Bhagat, S.K.; Tung, T.M.; Yaseen, Z.M. Development of artificial intelligence for modeling wastewater heavy metal removal: State of the art, application assessment and possible future research. *J. Clean. Prod.* **2019**, *250*, 119473. [CrossRef]
47. Garba, Z.N.; Ugbaga, N.I.; Abdullahi, A.K. Evaluation of optimum adsorption conditions for Ni (II) and Cd (II) removal from an aqueous solution by modified plantain peels (MPP). *Beni Suef Univ. J. Basic Appl.* **2016**, *5*, 170–179. [CrossRef]
48. Gupta, S.; Kumar, A. Removal of nickel (II) from an aqueous solution by biosorption on *A. Barbadensis* Miller waste leaves powder. *Appl. Water Sci.* **2019**, *9*, 96. [CrossRef]
49. ASTM D1293-18 Standard Test Methods for pH of Water. Available online: <https://www.astm.org/Standards/D1293.htm> (accessed on 15 June 2019).
50. Box, G.E.P.; Wilson, K.B. On the experimental attainment of optimum conditions. *J. R. Stat. Soc. Ser. B Methodol.* **1951**, *13*, 1–45. [CrossRef]
51. Lostado, R.; García, R.E.; Martínez, R.F. Optimization of operating conditions for a double-row tapered roller bearing. *Int. J. Mech. Mater. Des.* **2016**, *12*, 353–373. [CrossRef]
52. Lostado, R.; Escribano, R.; Martínez, M.A.; Múgica, R. Improvement in the design of welded joints of EN 235JR low carbon steel by multiple response surface methodology. *Metals* **2016**, *6*, 205. [CrossRef]
53. Harrington, E.C. The desirability function. *Ind. Qual. Control.* **1965**, *21*, 494–498.
54. Montgomery, D.C. *Design and Analysis of Experiments*; John Wiley & Sons: New York, NY, USA, 2008.
55. R Core Team. R: A Language and Environment for Statistical Computing. R Foundation for Statistical Computing. Available online: <https://www.r-project.org/> (accessed on 12 March 2019).
56. Lata, H.; Garg, V.K.; Gupta, R.K. Sequestration of nickel from an aqueous solution onto activated carbon prepared from *Parthenium hysterophorus* L. *J. Hazard. Mater.* **2008**, *157*, 503–509. [CrossRef] [PubMed]
57. Thirumavalavan, M.; Lai, Y.L.; Lee, Y.F. Fourier transform infrared spectroscopic analysis of fruit peels before and after the adsorption of heavy metal ions from an aqueous solution. *J. Chem. Eng. Data* **2011**, *56*, 2249–2255. [CrossRef]
58. Kandah, M.I.; Meunier, J.L. Removal of nickel ions from water by multi-walled carbon nanotubes. *J. Hazard. Mater.* **2007**, *146*, 283–288. [CrossRef]
59. Kuhn, M. Desirability: Desirability Function Optimization and Ranking. R package v.1.6. Available online: <http://CRAN.R-project.org/package=desirability> (accessed on 5 July 2019).

